Turkish Journal of Science & Technology
19(2), 497-508, 2024

Research Paper
https://doi.org/10.55525/tjst.1445681

Automatic Classification of Defective Photovoltaic Module Cells Based on a Novel CNN-PCA-SVM Deep Hybrid Model in Electroluminescence Images

Andaç İMAK[1*],
[1] Department of Electrical and Electronic Engineering, Faculty of Engineering, Munzur University, Tunceli, Turkey
[*1] andacimak@munzur.edu.tr

(Geliş/Received: 01/03/2024; Kabul/Accepted: 28/09/2024)

Abstract: In today's world, the rapid development of photovoltaic (PV) power plants has facilitated sustainable energy production. Maintenance and defect detection play crucial roles in ensuring the continuity of energy production. The manual inspection of electroluminescence (EL) images of PV modules requires significant human power and time investment. This study presents a method for the automatic fault detection of PV cells in EL images using hybrid deep features optimized with a principal component analysis (PCA) feature selection algorithm. A lightweight and high-performance model that combines the strengths of convolutional neural network (CNN) architectures was proposed. First, data augmentation techniques were employed owing to the imbalance between the defective and functional classes in the dataset containing EL images. In experimental studies conducted by integrating the PCA algorithm into MobileNetV2, DenseNet201, and InceptionV3 CNN models, accuracy, precision, recall, and F1-score values of 92.19%, 92%, 90%, and 91%, respectively, were achieved. When the results were analyzed, it was observed that the proposed method was effective in detecting faults in PV panel cells.

Key words: Deep learning, photovoltaic cells, defect detection, feature selection.

Yeni Bir CNN-PCA-SVM Derin Hibrit Modeline Dayalı Arızalı Fotovoltaik Modül Hücrelerinin Otomatik Sınıflandırılması

Öz: Günümüzde sürdürülebilir enerji üretimi için fotovoltaik (PV) enerji santrallerinin hızlı gelişimine olanak sağlamıştır. Enerji üretiminin sürekliliğinin sağlanması için bakım ve arıza tespiti önemli bir rol oynamaktadır. PV modüllerinin elektrolüminesans (EL) görüntülerinin manuel olarak incelenmesi, büyük bir insan gücü ve zaman yatırımını gerektirir. Bu çalışmada, EL görüntülerde PV hücrelerinin otomatik arıza tespiti için hibrit derin özniteliklerin, temel bileşenler analizi (PCA) öznitelik seçme algoritması ile optimize edilen bir yöntem sunmaktadır. Evrişimsel sinir ağı (CNN) mimarilerinin güçlü yönlerini birleştiren, hafif ve yüksek performanslı bir model önerilmektedir. İlk olarak EL görüntülerini içeren veri setindeki arızalı ve işlevsel sınıflarına ait veri dengesizliğinden dolayı veri arttırma teknikleri kullanılmıştır. MobileNetV2, DenseNet201 ve InceptionV3 CNN modellerine entegre edilen PCA algoritması ile hibrit kullanılarak gerçekleştirilen deneysel çalışmalarda doğruluk, kesinlik, duyarlılık ve F1-skoru değerleri sırasıyla %92.19, %92, %90 ve %91 olarak elde edilmiştir. Sonuçlar analiz edildiğinde, önerilen yöntemin PV panel hücrelerindeki arızaların tespitinde etkili bir performansa sahip olduğu gözlemlenmiştir.

Anahtar kelimeler: Derin öğrenme, fotovoltaik hücreler, kusur tespiti, özellik seçimi.

1. Introduction

The extensive utilization of fossil fuels has led to severe environmental pollution issues, resulting from an increase in carbon dioxide and other greenhouse gases in the atmosphere. This situation has triggered challenging global issues such as climate change, air pollution, and excessive use of natural resources. Therefore, the increasing energy consumption and demand for environmental protection underscore an urgent need for sustainable and clean energy sources. In recent years, there has been growing interest in renewable energy sources such as geothermal, hydroelectric, solar, and wind power. Renewable resources have emerged solutions capable of meeting energy needs while reducing environmental impacts [1], [2]. This transition plays a significant role in supporting environmental sustainability and contributes to a cleaner and more efficient future in the energy sector. Compared with wind energy systems, there has been a rapid increase in the interest and capacity of solar energy systems worldwide. Solar energy is one of the most attractive renewable energy sources because of its abundance, easy accessibility, and free usage [2], [3]. This situation is supported by the development of Photovoltaic (PV) technology for solar energy conversion and cost reduction.

PV modules, designed to last 25 years or longer, can experience various failure modes owing to environmental factors such as mechanical stress, humidity, high temperatures, and exposure to ultraviolet radiation. Consequently, these factors can degrade the solar cell performance even within the 25-year manufacturer warranty period [4], [5]. PV panels are typically installed outdoors with the assistance of aluminum frames and glass

[*] Corresponding author: andacimak@munzur.edu.tr. ORCID Number of authors: 0000-0002-3654-040X

lamination to protect them from environmental conditions. However, harsh climatic conditions and mechanical impacts during installation can lead to various failure modes, such as panel breakage, cracking, falling tree branches, snow accumulation, insect traces, burn marks, shading, and color changes. Additionally, manufacturing defects can also cause damage to PV panels, impeding the flow of current in PV systems and reducing the production capacity and efficiency. Therefore, effectively addressing the issues in solar energy technologies is crucial for ensuring sustainable and efficient energy production [6], [7], [8], [9].

Generally, the majority of solar power plants consist of thousands of modules with multi-megawatt (MW) capacity spread over large areas. However, monitoring this large number of modules individually is laborious and expensive. Studies reveal that long-term outdoor use of PV modules may be subject to premature failure due to a variety of factors, including lack of maintenance, enclosure issues, thermal cycling, grounding issues, and corrosive environments [10], [11], [12]. Efforts to identify power attenuation caused by microcracks in PV modules are going beyond traditional methods and are being strengthened by deep learning techniques. According to previous studies, microcracks can lead to a strength loss between 0.9% and 42.8% and cause hotspot effects [13], [14]. An advanced approach to detect such defects involves infrared thermal (IRT) imaging technology alongside I-V curve analysis [15]. However, the low resolution of these methods may limit the detection of microcracks that do not affect power efficiency.

High-resolution electroluminescence (EL) imaging systems have become an effective technology for defect detection in PV modules [16]. EL imaging offers a nondestructive approach capable of identifying microcracks and other defects with high resolution [17]. Defects in EL images typically manifest as dark grey lines and areas. However, the use of traditional methods to manually identify these defects is time consuming and may offer limited performance. In this context, deep learning techniques accelerate the processes of automatic defect detection and analysis, offering the potential to effectively identify microcracks in PV modules.

Owing to the powerful feature extraction capabilities of convolutional neural networks (CNNs), particularly in deep learning techniques, they have become increasingly popular for the detection of defects in EL images. Artificial intelligence models enable rapid detection of defects in EL images obtained over large areas, thereby streamlining the process. In the industrial field, there is a growing demand for deep architectural models that can satisfy the requirements of lightweight and effective detection networks in terms of both higher accuracy and speed in defect detection.

Research on the detection of surface defects in PV cells show an increasing trend. Tsanakas et al. in their study proposed the use of image histogram and Canny edge detector to detect defective cells through thermal images and separate these cells into specific regions. By applying the proposed method to two PV arrays mounted on a roof, they successfully detected 40 of the 43 defective cells [18]. Pratt et al. investigated the use of a U-Net-based semantic segmentation model of EL images to detect defects in solar PV modules. Their experimental results suggested that the trained U-net model can be used to quantify damage and determine the electrical performance during accelerated stress tests of PV modules [19]. Oliveira et al. conducted a study to detect defective PV modules in IRT images using a two-stage method comprising Laplacian-based edge detection and a CNN algorithm to segment defective solar panels. They classified defect detection using the developed neural network model into three categories [20]. Deitsch et al. used a CNN neural network model to detect defects on the surface of PV modules with EL images. They compared the results of the traditional machine learning method and the deep learning architecture, observing a 6% higher performance than the traditional machine learning method, with an accuracy score of 88.36% [21]. Tang et al. proposed a model using data augmentation and CNN architectures for automatic classification of defects in an EL image. To obtain a large number of high-resolution EL images, the generative adversarial network (GAN) image augmentation technique was utilized. An experimental study was subsequently conducted using the VGG16, ResNet50, Inception V3, and MobileNet architectures [22]. Hong et al. proposed a model containing YOLOv5 and the ResNet algorithm for defect detection in a PV module containing visible and infrared images. They observed that the proposed method significantly increased defect detection accuracy by up to 95% [23]. Zhao et al. proposed a CNN-based system for defect detection in PV modules that contains 19 types of defect classes to meet the inspection requirements of the production line. A dataset consisting of 5983 EL images was created, and using the labeled images, 19 different classes of defects were identified [24]. Sizkouhi et al. presented an autonomous fault-detection method that was developed to automatically detect common faults and defects that can be visually noticed in their work. The proposed network is based on a VGG16 model in an encoder-decoder architecture. Experimental studies have shown that the proposed network can precisely predict PV modules at the pixel level with an average accuracy of 98% and 93%, respectively [25]. There are studies examining the effectiveness of the YOLO algorithm for hotspot detection in PV modules and defect detection in solar power plants. There are studies examining the effectiveness of the YOLO algorithm for hotspot detection in PV modules and defect detection in solar power plants [26], [27], [28]. In this study, Açıkgöz and Korkmaz employed a transfer learning approach using SqueezeNet to create skip connections from the firing modules. They achieved a performance of 91.29% using the proposed method [29]. Demirci et al. compared the performances of these models using Alexnet, GoogleNet, MobilenetV2 and SqueezeNet transfer learning methods. Although the training load decreased with the transfer learning method, accuracy rates remained relatively low, between 76% and 79% [30]. In later years, Demirci et al. proposed an architecture in which 4 different deep learning architectures were used as a hybrid. In the PV dataset, they allocated 80% for training and 20% for testing for two classes. 5120 features were obtained with the deep network model, and 2000 sub-features were obtained with the minimum redundancy maximum relation (mRMR) algorithm. As a result of classification with machine learning methods such as support vector machine (SVM), k-nearest neighbour (KNN), decision tree (DT), random forest (RF) and naive bayes (NB), high accuracy rates of 94.52% were obtained for 2 classes (defective/functional) with the best performance SVM. In addition, a lightweight CNN architecture (L-CNN) they proposed in this study was trained from scratch without initial weights and achieved an accuracy rate of 89.33% [31].

Despite the utilization of advanced image processing and deep learning techniques in the literature, there are still many shortcomings in defect detection in PV modules. Therefore, efforts are being made to develop new methods to improve the reliability and efficiency of energy systems.

In this study, a deep learning-based classification method was proposed to detect faults in PV panel cells from EL images. The proposed method consists of a two-stage system that, includes deep learning architectures and a feature selection algorithm. The model provides a fast and simple fault detection method that utilizes effective deep learning architectures such as MobileNet V2, DenseNet201, and InceptionV3. Although MobileNetV2 stands out for its lightweight structure and high performance, DenseNet201 and InceptionV3 are deep network architectures capable of successfully handling large and complex feature spaces. In addition to the designed hybrid transfer learning approach, the integration of the principal component analysis (PCA) feature selection algorithm allows the model to focus on more effective and informative subset features, thus enhancing the usefulness of the method. The experimental studies resulted in an accuracy score of 92.19% with the proposed method. This hybrid model, reinforced with transfer learning approaches, provides a practical solution for classifying faults in PV panel cells with a fast implementation and more effective feature selection.

The remainder of this paper is organized as follows. In the first section, some information about the PV panel cells is presented. In the materials and methods section, detailed information is provided regarding the dataset used, deep models, feature selection algorithm, and architectural structure of the proposed model. The third section presents the experimental results. The final section presents the conclusions and potential future research directions.

2. Material and Methods

2.1. Dataset description and data augmentation

In this study, a dataset obtained from high-resolution EL images of both monocrystalline and polycrystalline PV panels was utilized [21], [32]. This publicly available dataset comprises 2624 EL images with a resolution of 300×300 pixels. It included 44 different PV panels, consisting of 18 monocrystalline and 26 polycrystalline panels. Among a total of 2624 images, 715 images are categorized as label 1 (defective), 295 images as label 0.66 (having surface defects), 106 images as label 0.33 (having minor defects without full faults), and 1508 images as label 0 (functional) without any detectable defects. Only the EL images with defective and functional labels were used in this study. The input images were resized to 224×224 pixels. Downsizing the input size helps optimize resource usage by reducing the computational workload. Figure 1 illustrates a few EL sample images belonging to defective and functional classes in the dataset used in the study.

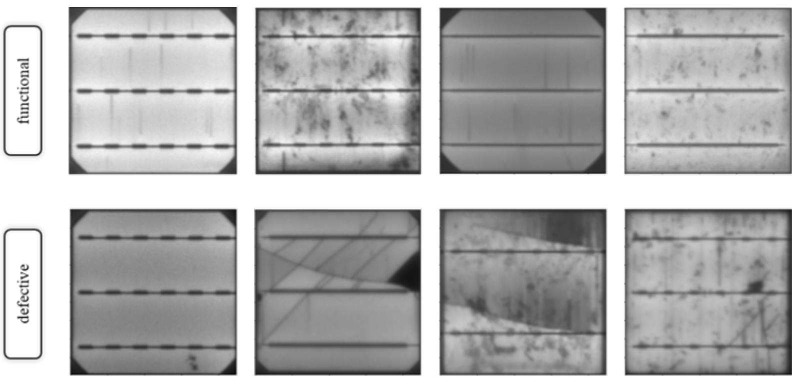

Figure1. Sample EL images of functional and defective classes

Data augmentation is a highly efficient technique for growing datasets with a small number of images. Effective data augmentation strategies can lead to a significant improvement in the system performance in image classification [33], [34]. The PV dataset edited in this study contained 2,223 EL images belonging to defective and functional classes. However, it is noteworthy that there are only 715 images for the defective class, which is less than half of the functional class. Because this unbalanced distribution may particularly affect the training performance of the proposed network, the number of samples needs to be increased. A system containing data augmentation techniques was used under Albumentation heading within Python libraries. The augmented synthetic images shown in Figure 2 were obtained by using horizontal flip, random rotation 90°, and vertical flip in the specified library for the images of the defective class in the training set.

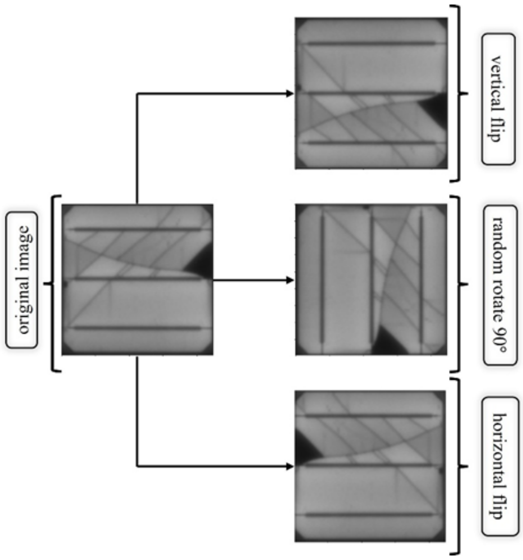

Figure 2. Synthetic images obtained with data augmentation techniques

2.2. Deep models and PCA

Deep learning architectures, such as InceptionV3, DenseNet201, and MobileNetV2, have proven their performance worldwide and have gained great popularity in recent years. These three architectures are known for their impressive success with large datasets. In particular, the InceptionV3 architecture is an improved and optimized version of the previous versions, InceptionV1 and InceptionV2. This architecture builds on previous models, such as GoogleNet by Szegedy et al. It provides versatile architecture that can successfully handle complex feature spaces [35]. The Dense201 model stands out because it optimizes the information transfer at the maximum level using dense connections. Dense connectivity is a structure in which the features obtained from each layer are connected to all the layers in the previous layer. This contributes to a more effective transfer of knowledge and to increases the learning capabilities of deeper networks [36], [37]. MobileNetV2 has a lightweight structure and effective performance in the field of CNN. This model is specifically designed for situations with resource constraints or application requirements. The proposed technique was based on the concept of MobileNetV2, an evolved version of MobileNet. MobileNetV2 offers a more effective and powerful convolutional neural network model by improving the features of the original MobileNetV1 [38].

Feature selection is the process of determining a subset that best represents the data and reduces the dimensionality while minimizing information loss. In this study, the principal component analysis (PCA) algorithm was used to find the most effective transformation that can express deep features with fewer variables. This method, proposed by Karl Pearson, minimizes information loss by determining the directions of the principal components while preserving the maximum variance without considering the class label. In this way, the representation of the data is strengthened, and the deep features analyzed are found in a more meaningful manner [39], [40].

2.3. Classification Method

Support Vector Machines (SVM) are a machine learning algorithm that generally separates data into different classes with a defined hyperplane. The primary objective of SVM is to identify the optimal hyperplane for data separation in classification tasks (as illustrated in Figure 3). The SVM algorithm, known for its success in classification and regression, aims to reduce generalization error when applied to unknown data [41].

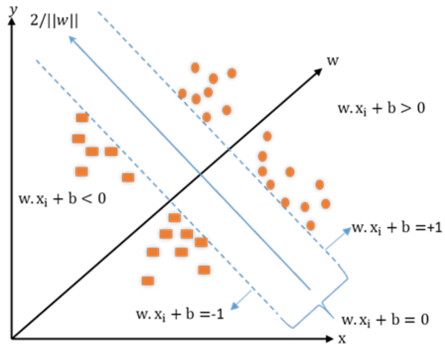

Figure 3. General illustration of SVM structure

The basic working principle of SVM is to keep the distance between the closest data points belonging to two classes at the maximum level. The higher the distance between the classes, the higher the classification performance. Suppose a d-dimensional dataset x(i) and an n-dimensional training set with binary class labels (-1,1). The SVM algorithm tries to obtain the hyperplane wx + b = 0 where the maximum level of the closest distance between the data points belonging to two classes is obtained [42].

The margin is defined as shown in Equation (1):

$$\text{Margin} = \frac{2}{||\text{w}||} \tag{1}$$

Here, w is the weight vector, ||·|| is the Euclidean norm of w. To maximize the hyperplane distance between classes, it is equivalent to minimizing ||w|| in accordance with the conditions outlined in Equation (2):

$$\begin{gathered} \min \frac{1}{2} ||\text{w}||^2 \\ \text{y}_\text{i}(w.\text{x}_\text{i} + \text{b}) \geq 1 \end{gathered} \tag{2}$$

The optimization problem can be solved by converting it into binary form using the Lagrange multipliers in Equation (3):

$$L(w, b, a) = \frac{1}{2} * \left|\left|\text{w}\right|\right|^2 - \sum a(i) * [y((i) * (w \cdot x(i) + b) - 1] \tag{3}$$

Here, a(i) represents the Lagrange multiplier. The most appropriate w (weight) and b(bias) values can be found by maximizing L(w,b,α), subject to the constraints α(i) ≥ 0 and ∑α(i) * y(i) = 0. SVM tries to define the hibernation plane separating positive and negative examples in linearly separable data. Also, in some classification problems, if the training data is not linearly separable, a kernel function is used to transform it to a higher dimensional space. Therefore, the non-linearly separable examples are transferred from the current space to various spaces with kernel functions such as radial basis function (RBF) and Gaussian [43], [44].

2.4. Proposed Method

In the proposed method, image augmentation techniques were first applied to the original dataset to ensure the optimal learning of CNN models. In the second step, the increased data were used as input to the proposed hybrid transfer learning methods consisting of MobileNetV2, DenseNet201, and InceptionV3 deep architectures. In addition, a global average pooling layer has been added to the last section to increase the representation ability of the features obtained from the transfer learning methods used. The PCA feature selection algorithm was applied separately to the various features obtained from the three different transfer learning models. The purpose of this step was to improve the representation of the feature set obtained from the model and to take advantage of the dimensionality reduction. As the second step in obtaining features from the model, the separated features were combined to obtain a more comprehensive perspective. These concatenated features were subjected to PCA. At this stage, feature selection was observed to play a critical role; therefore, a comprehensive analysis was conducted to determine the most appropriate feature subset. This analysis includes accuracy assessments performed with support vector machine (SVM) [41] applied to a series of values, starting from 50 and increasing the number of components by 25 to 500. This rigorous evaluation process was carried out to determine the best optimized values for the number of components of the PCA, regularization parameter (C) of the SVM, and coefficient (γ) of the RBF kernel. These optimum parameter values were used to obtain the ideal performance for the classifier model and ensure the accurate detection of faults in PV panel cells. Consequently, these new features were classified using the SVM algorithm, and a high-performance model was created to detect faults in PV panel cells. The block diagram of the proposed method is shown in Figure 4.

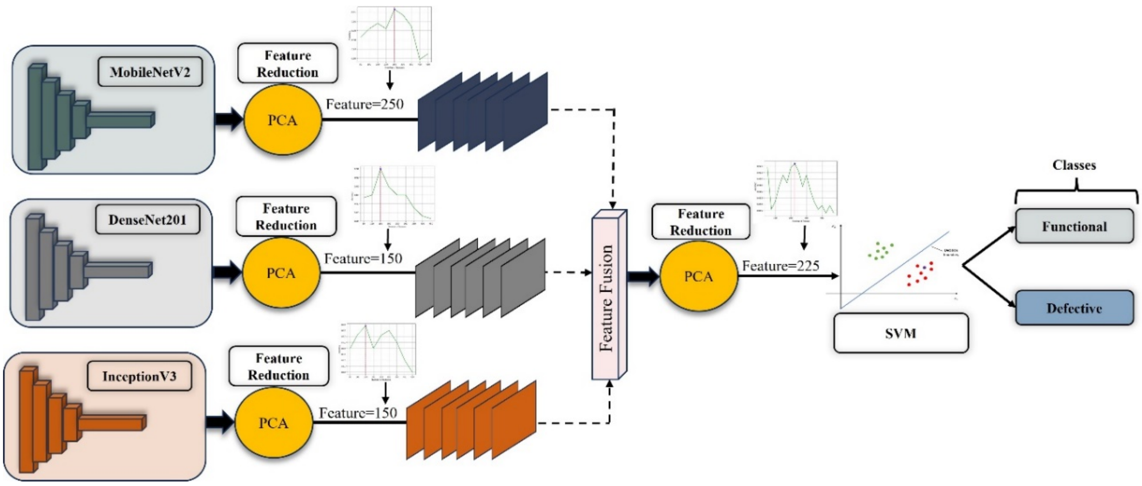

Figure 4. Block diagram of the proposed hybrid method

3. Experimental Results

In experimental studies, as a first step, 70% of the images in the data set are divided into training, 15% for testing, and 15% for validation. In a second step, data augmentation techniques were applied to the defective class section due to the irregularity between the defective and functional classes in the images allocated for training [45], [46], [47].

Performance metrics such as accuracy, precision, recall and F1-score were used to analyze the results obtained in the deep learning method proposed for PV cell defective detection. Performance metrics can be defined by the following mathematical Equations (4 to 7)

$$\text{Accuracy} = (\text{TP} + \text{TN})/(\text{TP} + \text{FN} + \text{TN} + \text{FP}) \tag{4}$$

$$\text{Precision} = \text{TP}/(\text{TP} + \text{FP}) \tag{5}$$

$$\text{Recall} = \text{TP}/(\text{TP} + \text{FN}) \tag{6}$$

$$\text{F1-score} = 2\,\text{TP}/(2\text{TP} + \text{FP} + \text{FN}) \tag{7}$$

It consists of 4 basic parameters obtained from the confusion matrices: true positive (TP), true negative (TN), false positive (FP) and false negative (FN).

Experimental studies on fault diagnosis in PV panel cells were carried out meticulously using state-of-the-art software such as Python 3.7.13, Tensorflow 2.8.0 and Keras 2.8.0. In addition, it was compiled using hardware technologies such as Intel(R) Xeon(R) CPU @ 2.30GHz, 27.6 GB RAM, Tesla T4- 16. During the training process, the epoch size was determined as 100 and the batch size was 16. The 'Adam' optimization method was used with a learning rate of 0.0001. The initial learning rate was set to 0.0001, and when the validation loss did not decrease after 10 epochs, the learning rate was reduced to 0.00001 using ReducLROnPlateau. Binary crossentropy loss function was used in these models. These adjustments were carefully selected to achieve optimal training results for PV panel cell defective classification. The hyperparameters used in the MobileNetV2, DenseNet 201 and InceptinV3 CNN models are given in Table 1.

Table 1. Hyper-parameter values used in hybrid-CNN models

CNN models	Image Size	Optimization Methods	Momentum	Epoch	Mini Batch	Learning Rate
MobileNetV2	224×224	Stochastic Gradient Descent	0.9	50	16	1e-4
DenseNet 201						
InceptionV3						

As shown in the block diagram given in Figure 4, the proposed approach consists of three main stages: extraction of deep features, feature selection, and classification. The study analyzes how the hybrid use of transfer learning methods and the inclusion of feature selection algorithms contribute to the overall success. In the task of feature extraction, these CNN models utilize a global average pooling layer for their outputs, aiming to maintain the learning levels of the CNN model optimally. The curves of the proposed MobileNetV2, DenseNet201, and InceptionV3 transfer learning methods are shown in Figure 5. Figure 5 illustrates the training (in red) and validation accuracy curves (in green). It also includes loss and accuracy curves for both the training and validation sets.

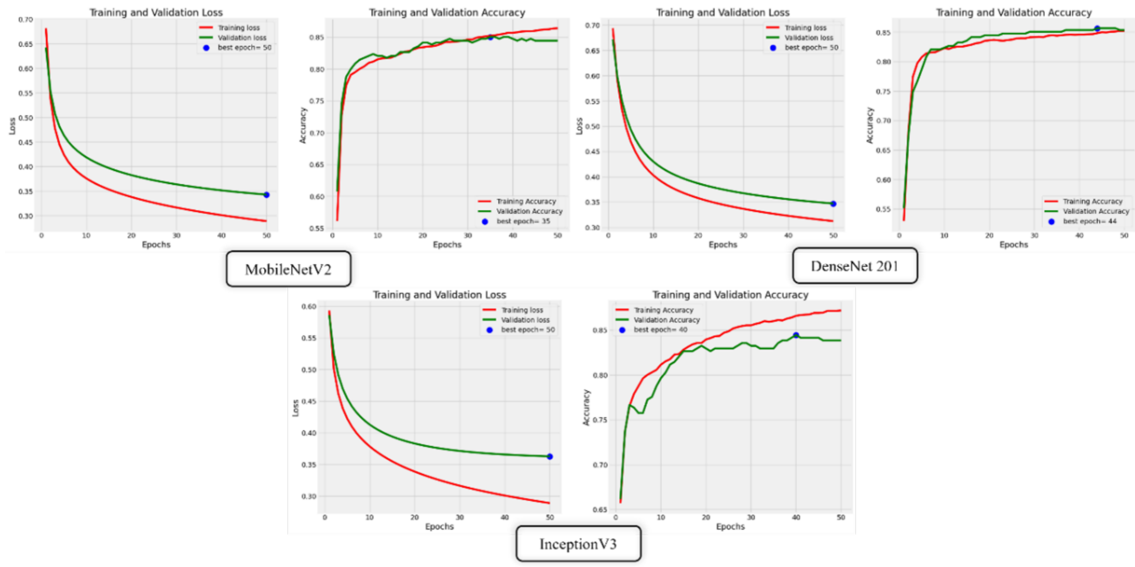

Figure 5. Loss and accuracy graphs obtained with the proposed deep architectures

As seen in Figure 5, training accuracies increased by over 80% in the first few steps, and similarly training loss values regularly dropped below 0.5. In the first stage, the features obtained from the last layer (global average pooling) of three different transfer learning methods, namely MobileNetV2, DenseNet 201 and InceptinV3, without including the PCA feature selection algorithm, and the results of classifying these features with the SVM classification algorithm are shown in Table 2.

Table 2. Results of the proposed methods (a system where PCA is not used)

CNN models+SVM	Accuracy	Precision	Recall	F1-score
MobileNetV2	0.84	0.82	0.84	0.83
DenseNet 201	0.84	0.82	0.83	0.83
InceptionV3	0.85	0.83	0.85	0.84

When referring to Table 2, it becomes evident that in the three transfer learning methods, MobileNetV2 and DenseNet 201 achieved similar performance results with 84% accuracy, 82% precision, approximately 84% recall, and 83% F1-score. On the other hand, the InceptionV3 CNN model outperformed the other two methods with 85% accuracy, 83% precision, 85% recall, and 84% F1-score values, showing a 1% higher performance. These results are important to understand the effectiveness between the models.

In the second stage, PCA feature selection algorithm was employed to obtain the best feature subset from the features obtained from three different transfer learning methods: MobileNetV2, DenseNet 201 and InceptinV3. To optimally select the number of components, which is a determining parameter of PCA, the number of components was determined to be 50, and the feature and accuracy values were observed to obtain the highest level of performance with a technique that increased by 25 to 500. At the end of this meticulous process, the most effective number of components was determined to be 250, 150, and 150 for MobileNetV2, DenseNet201, and InceptionV3, respectively, as illustrated in Figure 6. Maximum performance results according to the features in the system where the PCA feature selection algorithm and the SVM classifier are integrated are given in Table 3.

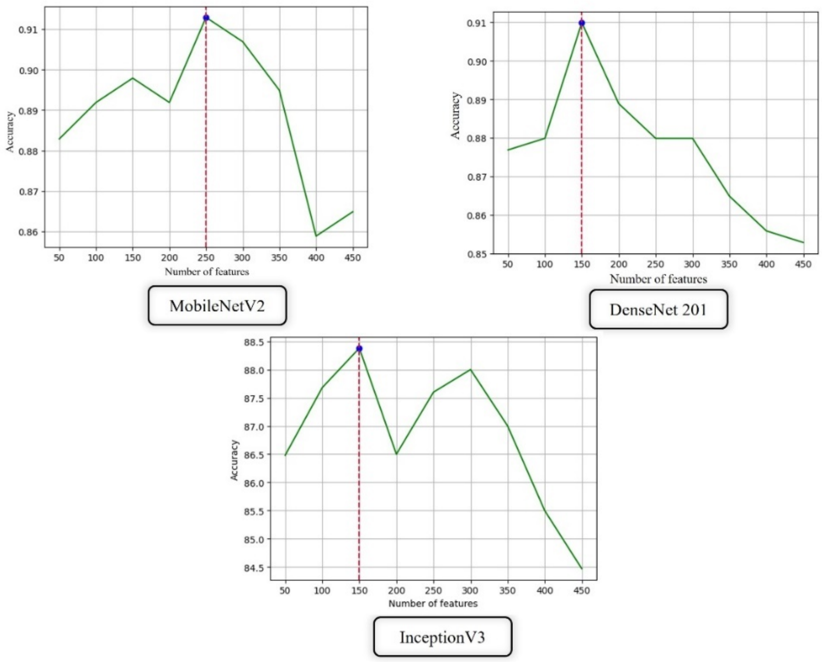

Figure 6. Accuracy graphs according to the number of features of 3 different CNN models

Table 3. Results of the proposed methods (a system integrated with PCA)

Models	Number of features	Classification	Accuracy
MobileNetV2	250		0.9129
DenseNet201	150	SVM	0.9099
InceptionV3	150		0.8838

The obtained features were classified using an SVM classifier, and the confusion matrices resulting from SVM classification are presented in Figure 7. According to the results in Table 3, applying the PCA feature selection algorithm to CNN models yielded accuracy results of 91.29% for MobileNetV2, 90.99% for DenseNet201, and 88.28% for InceptionV3. Upon observation of the results, it is evident that the features selected by PCA optimize the representation capabilities, allowing for the differentiation of defective and functional PV cell samples. The SVM algorithm effectively distinguishes between defective and functional cells by classifying these features. Comparing these results with Table 2, MobileNetV2 exhibited 7.29%, DenseNet201 showed 6.99%, and InceptionV3 displayed 3.28% higher accuracy performance. Detailed confusion matrices resulting from the PCA feature selection algorithm integrated into three separate CNN models are detailed in Figure 7.

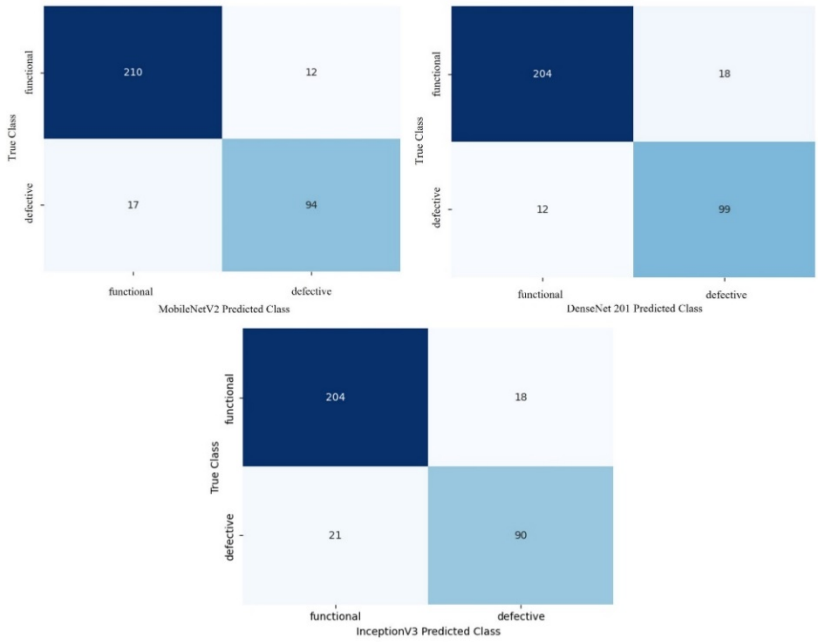

Figure 7. Confusion matrices obtained with feature subset

The performance metrics obtained at each stage of the proposed model shed light on the strengths and weaknesses of the transfer learning methods integrated for defect detection in EL images. These experimental results aim to help researchers choose the most appropriate transfer learning approach for similar tasks.

In the final stage of the experimental study, features detailed from the MobileNetV2, DenseNet201, and InceptionV3 CNN models, as elaborated in Figure 6, were combined to create 550 new feature subsets for each image. To focus on a more effective and informative subset of features, the PCA algorithm was applied again. In Figure 8, a graph of accuracy is presented based on the number of components detailed in the previous step, aiming to determine the best subset component count from the merged features. In addition, Figure 8 shows in detail the confusion matrices obtained from the classification of the best features by the SVM algorithm.

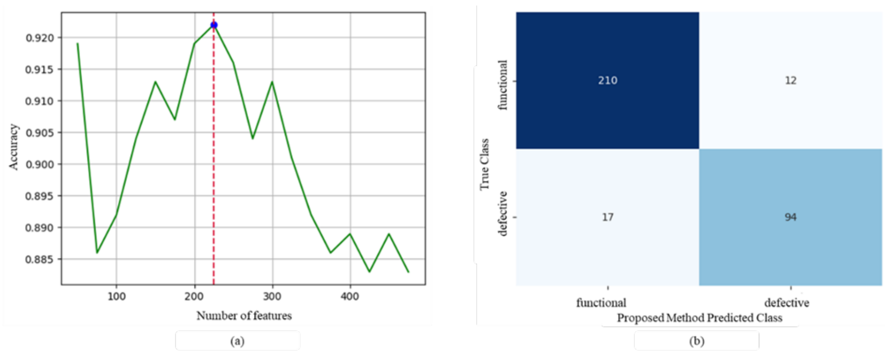

Figure 8. The proposed model; (a) accuracy plot according to the number of features, (b) confusion matrices

The performance metrics calculated with confusion matrices obtained from experimental studies using the proposed combination of fusion, PCA, and SVM are presented in Table 4. Upon evaluating the performance results obtained, the proposed method demonstrated superior performance compared to other results. Additionally, it is compared with the two-class (functional/defective) study conducted by Açıkgöz and Korkmaz [29] using the same dataset, as shown in Table 5. Both studies utilized the same training, testing, and validation rates for the two-class dataset. When the performances were compared for 70% training, 15% testing, and 15% validation, the proposed method exhibited approximately 1% higher performance using 225 features. This literature comparison highlights the importance and effectiveness of the proposed method. Furthermore, Demirci et al. [31], who employed the same dataset in their study, divided the dataset into 80% for training and 20% for testing. They achieved accuracies of 89.33% and 94.52%, respectively, with the L-CNN and deep feature-based SVM (DFB-SVM) methods proposed in their study. Upon observing the performance results of 2000 features produced using the DFB-SVM approach described by Demirci et al. [31], performance results close to these were obtained with 225 features generated using the proposed method. However, it is not appropriate to compare the performance of the proposed model with previous studies where separated datasets for training and testing were used in different proportions. Dataset sections used in different proportions may affect the model's performance and may not be suitable for an accurate comparison.

Table 4. The results of the proposed Hybrid CNN-PCA method

CNN models	Accuracy	Precision	Recall	F1-score
Proposed method	0.9219	0.92	0.90	0.91

Table 5. The comparison of the proposed method with the method using the same dataset

CNN models	Accuracy	Precision	Recall	F1-score
Açıkgöz and Korkmaz [29]	0.9129	0.8421	0.8972	0.8688
Proposed method	**0.9219**	**0.92**	**0.90**	**0.91**

4. Conclusion

In this study, an improved transfer learning method is presented for effective detection of faults in PV panel cells. PCA algorithm was integrated separately using widely preferred deep learning models such as MobileNetV2, DenseNet201 and InceptionV3. In the next stage, the resulting feature subsets were combined and processed again with the PCA algorithm. This approach aims to benefit from information at different scales while preserving the unique attributes of each model. The obtained features were processed with the SVM algorithm and the defects in PV panel cells were classified. As a result of the experimental studies, an accuracy rate of 92.19% was achieved. The proposed method performed approximately 1% better than the study conducted using the same dataset in the literature.

In future studies, it is aimed to optimize this method for defective detection in the cells of PV panels and to enable it to work in real time on embedded systems. Additionally, it is planned to contribute to the literature by creating a more comprehensive PV panel dataset.

Reference

[1] Pillai DS, and Rajasekar N. A comprehensive review on protection challenges and fault diagnosis in PV systems. Renewable and Sustainable Energy Reviews, 2018; 91:18–40.
[2] Eltamaly AM. A novel benchmark shading pattern for PV maximum power point trackers evaluation. Sol Energy, 2023; 263:111897.
[3] Demir A, Dinçer AE, and Yılmaz K. A novel method for the site selection of large-scale PV farms by using AHP and GIS: A case study in İzmir, Türkiye. Sol Energy, 2023;259:235–245.
[4] Omazic A et al. Relation between degradation of polymeric components in crystalline silicon PV module and climatic conditions: A literature review. Sol Energy Mater Sol Cells, 2019;192:123–133.
[5] Vázquez M, and Rey-Stolle I. Photovoltaic module reliability model based on field degradation studies. Prog Photovoltaics Res Appl, 2008;16(5):419–433.
[6] Silvestre S, Kichou S, Chouder A, Nofuentes G, and Karatepe E. Analysis of current and voltage indicators in grid connected PV (photovoltaic) systems working in faulty and partial shading conditions. Energy, 2015;86:42–50.
[7] Dhoke A, Sharma R, and Saha TK. PV module degradation analysis and impact on settings of overcurrent protection devices. Sol Energy, 2018;160:360–367.
[8] Wang H, Zhao J, Sun Q, and Zhu H. Probability modeling for PV array output interval and its application in fault diagnosis. Energy, 2019;189:116248.
[9] Gong B, An A, Shi Y, and Zhang X. Fast fault detection method for photovoltaic arrays with adaptive deep multiscale feature enhancement. Appl Energy, 2024;353:122071.
[10] Munoz MA, Alonso-García MC, Vela N and Chenlo F. Early degradation of silicon PV modules and guaranty conditions. Sol Energy, 2011;85(9):264–2274.
[11] Djordjevic S, Parlevliet D, and Jennings P. Detectable faults on recently installed solar modules in Western Australia. Renew Energy,2014; 67:215–221
[12] Dhoke A, Sharma R, and Saha TK. PV module degradation analysis and impact on settings of overcurrent protection devices. Sol. Energy, 2018;160:60–367.

[13] Dhimish M. Micro cracks distribution and power degradation of polycrystalline solar cells wafer: Observations constructed from the analysis of 4000 samples. Renew Energy, 2020;145:466–477.
[14] Abdelhamid M, Singh R, and Omar M. Review of microcrack detection techniques for silicon solar cells. IEEE J Photovolt, 2014;4(1):514–524.
[15] Tsanakas JA, Ha L, and Buerhop C. Faults and infrared thermographic diagnosis in operating c-Si photovoltaic modules: A review of research and future challenges. Renewable Sustainable Energy Rev., 2016;62:695–709.
[16] Fuyuki T, and Kitiyanan A. Photographic diagnosis of crystalline silicon solar cells utilizing electroluminescence. Appl Phys A Mater Sci Process,2009;96(1):189–196.
[17] Breitenstein O et al. Can luminescence imaging replace lock-in thermography on solar cells. IEEE J Photovolt, 2011;1(2):159–167.
[18] Tsanakas JA, Chrysostomou D, Botsaris PN, and Gasteratos A. Fault diagnosis of photovoltaic modules through image processing and Canny edge detection on field thermographic measurements. Int J Sustainable Energy, 2013;34(6):351–372.
[19] Pratt L, Govender D, and Klein R. Defect detection and quantification in electroluminescence images of solar PV modules using U-net semantic segmentation. Renew Energy, 2021;178:1211–1222.
[20] Vidal De Oliveira AK, Rüther R, and Aghaei M. Automatic Fault Detection of Photovoltaic Arrays by Convolutional Neural Networks During Aerial Infrared Thermography. In Proceedings of the 36th European Photovoltaic Solar Energy Conference and Exhibition,2019;9-13.
[21] Deitsch S et al. Automatic classification of defective photovoltaic module cells in electroluminescence images. Sol Energy, 2019;185:455–468.
[22] Tang W, Yang Q, Xiong K, and Yan W. Deep learning based automatic defect identification of photovoltaic module using electroluminescence images. Sol Energy, 2020;201:453–460.
[23] Hong F, Song J, Meng H, Rui W, Fang F, and Guangming Z. A novel framework on intelligent detection for module defects of PV plant combining the visible and infrared images. Sol Energy, 2022;236:406–416.
[24] Zhao Y, Zhan K, Wang Z, and Shen W. Deep learning-based automatic detection of multitype defects in photovoltaic modules and application in real production line. Prog Photovoltaics Res Appl., 2021;29(4):471–484.
[25] Moradi Sizkouhi A, Aghaei M, and Esmailifar SM. A deep convolutional encoder-decoder architecture for autonomous fault detection of PV plants using multi-copters. Sol Energy, 2021;223:217–228.
[26] Sun T, Xing H, Cao S, Zhang Y, Fan S, and Liu P. A novel detection method for hot spots of photovoltaic (PV) panels using improved anchors and prediction heads of YOLOv5 network. Energy Reports, 2022;8:1219-1229.
[27] Yanilmaz S, Türkoğlu M, and Aslan M. Güneş enerjisi santrallerinde YOLO algoritmaları ile hotspot kusurlarının tespiti. Fırat University Journal of Engineering Science, 2024;36(1):121-132.
[28] Cao Y, et al. Improved YOLOv8-GD deep learning model for defect detection in electroluminescence images of solar photovoltaic modules, Eng Appl Artif Intell, 2024;131:107866.
[29] Açikgöz H, and Korkmaz D. Elektrolüminesans görüntülerde arızalı fotovoltaik panel hücrelerin evrişimli sinir ağı ile otomatik sınıflandırılması. Fırat University Journal of Engineering Science, 2022;34(2):589–600.
[30] Demirci MY, Beşli N, and Gümüşçü A. Defective PV cell detection using deep transfer learning and EL imaging. In International Conference on Data Science, Machine Learning and Statistics 2019 (DMS-2019), 2019;311–314.
[31] Demirci MY, Beşli N, and Gümüşçü A. Efficient deep feature extraction and classification for identifying defective photovoltaic module cells in Electroluminescence images, Expert Syst Appl, 2021;175:114810.
[32] Deitsch S et al. Segmentation of photovoltaic module cells in uncalibrated electroluminescence images. Mach Vis Appl, 2021;32(4):1–23.
[33] Imak A, Celebi A, Siddique K, Turkoglu M, Sengur A, and Salam I. Dental caries detection using score-based multi-input deep convolutional neural network. IEEE Access, 2022;10:18320–18329.
[34] Turkoglu M. COVIDetectioNet: COVID-19 diagnosis system based on X-ray images using features selected from pre-learned deep features ensemble. Appl Intell, 2021;51(3)1213–1226.
[35] Szegedy C, Vanhoucke V, Ioffe S, Shlens J, and Wojna Z. Rethinking the inception architecture for computer vision. In Proceedings of the IEEE conference on computer vision and pattern recognition, 2016;2818–2826.
[36] Wang SH, and Zhang YD. DenseNet-201-based deep neural network with composite learning factor and precomputation for multiple sclerosis classification. ACM Transactions on Multimedia Computing, Communications, and Applications (TOMM), 2020;16(2).
[37] Turkoglu M, Hanbay D, and Sengur A. Multi-model LSTM-based convolutional neural networks for detection of apple diseases and pests. J Ambient Intell Humaniz Comput, 2022;13(7):3335–3345.
[38] Sandler M, Howard A, Zhu M, Zhmoginov A, and Chen LC. MobileNetV2: Inverted residuals and linear bottlenecks, 2018;4510–4520.
[39] Pearson K. LIII. On lines and planes of closest fit to systems of points in space. The London, Edinburgh, and Dublin Philosophical Magazine and Journal of Science, 1901; 2(11):559–572.
[40] İmak A, Doğan G, Şengür A, and Ergen B. Asma Yaprağı türünün sınıflandırılması için doğal ve sentetik verilerden derin öznitelikler çıkarma, birleştirme ve seçmeye dayalı yeni bir yöntem. International Journal of Pure and Applied Sciences, 2023;9(1):46–55.
[41] Cortes C, and Vapnik V. Support-vector networks. Mach Learn, 1995;20(3):273–297.
[42] Serin J, Vidhya KT, Deepa IMI, Ebenezer V, and Jenefa A. Gender classification from fingerprint using hybrid CNN-SVM. Journal of Artificial Intelligence and Technology, (2024);4(1):82-87.

[43] Demir F. DeepBreastNet: A novel and robust approach for automated breast cancer detection from histopathological images. Biocybernetics and biomedical engineering, (2021);41(3):1123-1139.
[44] Polat H, Türkoğlu M, Polat O, and Şengür A. A novel approach for accurate detection of the DDoS attacks in SDN-based SCADA systems based on deep recurrent neural networks. Expert Systems with Applications, (2022);197:116748.
[45] Doğan G, and Ergen B. A new mobile convolutional neural network-based approach for pixel-wise road surface crack detection. Measurement, 2022;195:111119.
[46] Doğan G, and Ergen B. Karayollarındaki asfalt çatlaklarının tespiti için yeni bir konvolüsyonel sinir ağı tabanlı yöntem. Fırat University Journal of Engineering Science, 2022;34(2):485–494.
[47] Imak A, Çelebi A, Polat O, Türkoğlu M, and Şengür A. ResMIBCU-Net: an encoder–decoder network with residual blocks, modified inverted residual block, and bi-directional ConvLSTM for impacted tooth segmentation in panoramic X-ray images. Oral Radiol., 2023;1:1–15.